LARGE-SCALE PHOTOEVAPORATION FLOWS IN H II REGIONS

W. J. Henney

Instituto de Astronomía, Universidad Nacional Autónoma de México, Morelia, México

RESUMEN

Presento modelos analíticos sencillos para flujos fotoevaporados estacionarios en el tiempo en regiones H II. Se consideran dos casos: (1) un flujo globalmente abierto de un frente de ionización plano, en donde la fuente ionizadora se encuentra a una distancia finita del frente; (2) flujos locales de las cimas de ondulaciones en el frente de ionización dentro de una región H II globalmente cerrada. Muestro que el primer caso reproduce bién la geometría y propiedades físicas observadas de la capa principal de emisión de líneas ópticas en la nebulosa de Orión, mientras que el segundo caso puede explicar naturalmente el aumento en la densidad ionizada, lo cual está observado en el entorno de la barra de Orión.

ABSTRACT

I present simple analytic models for steady-state photoevaporation flows in H II regions. Two cases are considered: (1) the globally open flow from a plane ionization front, where the ionizing source is offset a finite distance from the front; (2) local flows from the crests of ionization-front undulations in a globally closed H II region. I show that the first case can well reproduce the observed geometry and physical properties of the principal optical line-emitting layer in the inner Orion nebula, while the second case can naturally explain the observed ionized density increase in the vicinity of the Orion bar.

Key Words: **H II REGIONS** — **HYDRODYNAMICS** — **ISM: INDIVIDUAL (ORION NEBULA)**

1. INTRODUCTION

The rich, varied, and spectacular structure and kinematics shown by optically visible, compact to giant H II regions has long been the subject of intense observational study—see O'Dell (2001, Orion nebula), Hester et al. (1996, Eagle nebula), Smith et al. (2000, Carina nebula), Moffat et al. (2002, NGC 3603), Walborn & Maíz-Apellániz (2002, 30 Dor), and references therein. An impressive amount of theoretical modeling has also been carried out. Pioneering early work is described in Yorke (1986) with more recent contributions from García-Segura & Franco (1996) and Williams, Ward-Thompson, & Whitworth (2001). However, the fundamental structure and kinematics of the Orion nebula, the best-studied of all these regions, have never been satisfactorily explained by theoretical models. I here present a first attempt at plugging this gap, drawing on the concept of the photoevaporation flow, which has recently been successfully applied to the Orion proplyds and to cometary knots in planetary nebulae (see O'Dell et al. 2002; Henney et al. 2002, and references therein).

2. PHOTOEVAPORATION FLOW FROM A PLANE IONIZATION FRONT

Consider an infinite plane ionization front ($z = 0$) illuminated by a point source of ionizing radiation, which lies at a height $z = z_*$ above the i-front and defines the cylindrical axis $r = 0$ (see Figure 1). Suppose that the i-front is everywhere D-critical and that the volume $z > 0$ is filled with a time-steady,[1] isothermal, ionized photoevaporation flow with straight streamlines. Each streamline can be labeled with the cylindrical radius r_0 of its footpoint on the i-front and makes an angle $i(r_0)$ with the z-direction. Assume that the acceleration of the flow along a streamline is identical to that in the photoevaporation flow from a spherical globule with a radius equal to the local "divergence radius" of the flow: $R_d = r_0 \csc i$. Hence, the velocity along each streamline follows an identical function $U(y) \equiv u/c_i$, where $y = 1 + s/R_d$, s is the distance along the streamline, and c_i is the isothermal sound speed in the ionized gas (since the front is D-critical, we have $U(0) = 1$). The density at any point (r, z) can therefore be separated as

$$n(r, z) = \frac{N(r_0)}{y^2 U(y)}, \qquad (1)$$

where $r = r_0 + (y-1)R_d \sin i$ and $z = (y-1)R_d \cos i$.

The recombination scale height along a streamline, $h(y_0)$, is defined as the thickness of an equiv-

---

[1] The steady-state assumption can be justified by the observation that the gas velocity in the photoevaporation flow will be several hundred times higher than the propagation speed of a D-critical i-front into 100 K neutral gas.
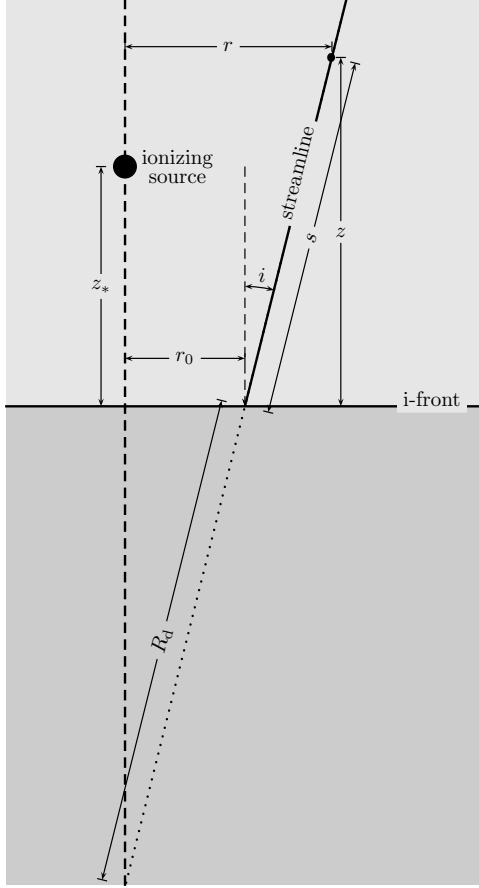
Fig. 1. Schematic diagram of the photoevaporation flow from a plane ionization front illuminated by a point source, in which the principal geometrical quantities are indicated.

alent homogeneous layer of density $N(r_0)$ that has the same recombination rate per unit area as the entire flow along the streamline: $N^2(r_0)h = \int_0^\infty n^2(r_0, s)\, ds$, yielding

$$h = R_d \int_1^\infty y^{-4}U^{-2}\, dy = \omega R_d, \qquad (2)$$

where ω is a constant that depends only on the acceleration law $U(y)$ ($\omega \simeq 0.1$ for typical photoevaporation flows, Bertoldi 1989).

With this definition of h, and assuming that the photoevaporation flow is "recombination dominated" (Henney 2001), that recombinations can be treated in the on-the-spot approximation, and ignoring any absorption of ionizing photons by grains, one can approximate the recombination/ionization balance along a line from the ionizing source to the i-front by considering the perpendicular flux of ionizing photons incident on the equivalent homogeneous layer:

$$\frac{Q_H \cos\theta}{4\pi(z_*^2 + r_0^2)} = \alpha_B N^2(r_0)h(r_0), \qquad (3)$$

where $\tan\theta = r_0/z_*$, Q_H is the ionizing photon luminosity (s^{-1}) of the source, and α_B is the Case B recombination coefficient. This approximation will be valid when h is small enough to satisfy $h < z_*$ and $h\sec\theta < H$, where $H \equiv |d\ln N/dr_0|^{-1}$ is the radial scale length of the ionized density profile at the i-front. This profile can be found from equation (3) to be

$$N(r_0) = N_0(1 + x^2)^{-3/4}(h/h_0)^{-1/2}, \qquad (4)$$

where $x = r_0/z_*$ and N_0, h_0 are the values on the axis at $r_0 = 0$. Note that for any plausible $h(r_0)$, the density at the i-front will decrease with increasing radius.

In order to complete the solution, it is now only necessary to specify the radial dependence of the streamline angle, $i(r_0)$, from which the radius of divergence, $R_d(r_0)$ and scale height, $h(r_0)$, follow automatically. To do this, we must recognise that the streamlines cannot truly be straight: in a D-critical front the gas will be accelerated up to the ionized sound speed, c_i, in the z-direction (perpendicular to the front) but at $z = 0$ it will have no velocity in the r-direction (parallel to the front). However, the pressure gradient associated with the radially decreasing density will laterally accelerate the gas in the positive r-direction as it rises through the recombination layer (which is much thicker than the front itself), thus bending the streamlines outwards. To be definite, we will consider the characteristic angle of each streamline, $i(r_0)$, to be that obtained by the gas at $z = h(r_0)$.

The lateral acceleration, a, of the gas is given by

$$a = \frac{1}{\rho}\frac{dP}{dr} = \frac{c_i^2}{H}, \qquad (5)$$

where H is the lateral density scale length defined above. Ignoring the vertical acceleration of the gas, the time taken to rise to a height h is h/c_i, so that the lateral speed reached is $c_i h/H$ and the streamline angle is given by

$$\tan i = \frac{h}{H}, \qquad (6)$$

so that $R_d = h/\omega = r_0(1 + H^2/h^2)^{1/2}$. In the limit that $h^2/H^2 \ll 1$, this can be solved to give

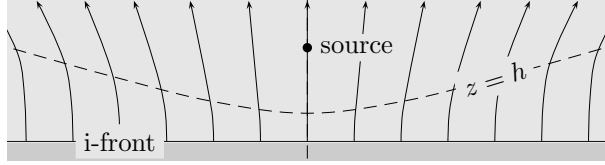$$h \simeq (\omega H r_0)^{1/2}. \qquad (7)$$

Fig. 2. Photoevaporation flow solution for the plane ionization front. Streamlines are indicated by arrows and the vertical scale height of the flow is shown by the dashed line.

From equation (4), we find

$$\frac{d \log N}{dr_0} = -\frac{3}{4}\frac{r_0}{z_*^2 + r_0^2} - \frac{1}{2}\frac{d \log h}{dr_0}, \qquad (8)$$

from which we can obtain $H \simeq r_0 + z_*^2/r_0$ by ignoring the second term and the factor of $\frac{3}{4}$ in the first term (we will return to this later). Substituting this value for the lateral scale length into equation (7), we finally obtain

$$h \simeq \left[\omega\left(z_*^2 + r_0^2\right)\right]^{1/2} \simeq 0.346z_*(1 + x^2)^{1/2}, \qquad (9)$$

which may in turn be substituted back into equation (4) to give

$$N(r_0) = N_0(1 + x^2)^{-1}. \qquad (10)$$

Note that this final form for the radial density profile does give the exact result $H = r_0 + z_*^2/r_0$, hence justifying the maneuver made after equation (8) above. From equation (6), the streamline angles are given by

$$\tan i = 0.346x(1 + x^2)^{-1/2}. \qquad (11)$$

Hence, the vertical scale height on the axis is given by $h_0 = 0.346z_*$, at which point the streamlines are vertical. Moving away from the axis, the streamlines start to diverge slightly, reaching an asympotic angle of $i_\infty = \tan^{-1} 0.346 \simeq 19°$ as $r_0 \to \infty$. The general flow pattern is shown in Figure 2. Note that since h/H is everywhere smaller than 0.346, the approximation leading to equation (7) above is justified.

The most serious simplification in the present treatment of the problem is the assumption of straight streamlines in deriving the density profile along the streamlines, together with the arbitrariness in specifying the streamline angle to be that achieved at $z = h$. As a result, the exact value of the factor 0.346 in the above results should be treated with caution. Also, the validity of the results for r_0 greater than a few times z_* is doubtful, since h no longer satisfies the conditions stated after equation (3) above. It will be interesting to compare
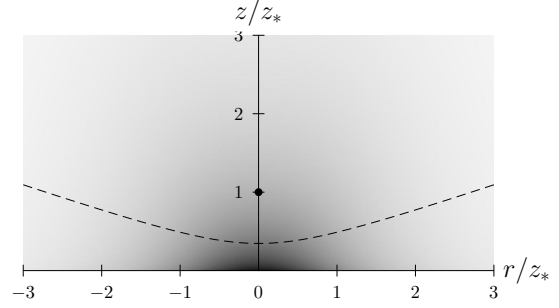

Fig. 3. Resultant density distribution from the photoevaporation flow from a plane ionization front. The scale is linear, from $n(0,0)$ (black) to zero (white). The position of the ionizing star is shown by a filled circle. The dashed lines shows the vertical scale height, h, from equation (9).
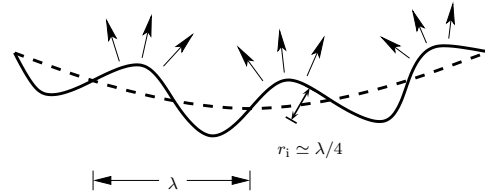

Fig. 4. A globally concave i-front (dashed line) is perturbed by a large-amplitude undulation with wavelength λ. The i-front curvature is now convex at the crests of the undulation, allowing the possibility of local divergent photoevaporation flows.

this approximate flow solution with the results of a more exact treatment of the dynamics obtained from a numerical hydrodynamics simulation.

3. PHOTOEVAPORATION FLOWS FROM AN UNDULATING IONIZATION FRONT

In the previous section, it was shown that one can obtain a self-consistent description of a photoevaporation flow from a plane i-front illuminated by a point source. However, the solution obtained depends critically on the assumption of a *globally open* geometry, allowing the gas to flow freely away from the ionization front. Is it possible for photoevaporation flows to exist inside an H II region with a *globally closed* geometry, such as a classical Strömgren sphere? The only possibility would seem to be if the i-front were irregular on some scale, λ, giving localized regions with convex curvature, from which a divergent photoevaporation flow could be established as shown in Figure 4. The radius of curvature of the crests of the undulation will be $r_i \simeq \lambda/4$ so long as their amplitude is $\geq \lambda/4$.

First, consider an idealized homogeneous Strömgren sphere of radius R_0 and density n_0 that sur-
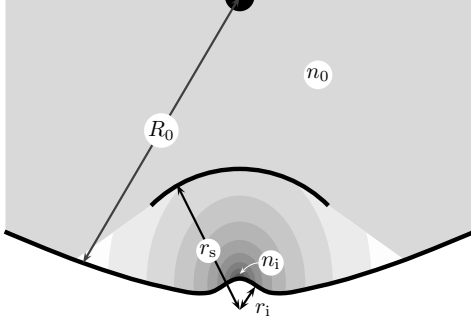
Fig. 5. The photoevaporation flow from the crest of an undulation in the i-front of a spherical homogeneous H II region of radius R_0. The flow carves out a cavity of radius r_s.

rounds a star with ionizing photon luminosity Q_H. The global ionization balance equation is

$$\frac{4}{3}\pi R_0^3 n_0^2 \alpha_B = Q_H, \qquad (12)$$

where α_B is the recombination coefficient. Now, consider a large-amplitude undulation of the ionization front with wavelength λ as described above. Assume that the IF at the crest of the undulation is approximately D-critical and that a steady-state photoevaporation flow streams off it. We will consider both spherically divergent flows, as would be expected from the head of a pillar, and cylindrically divergent flows, as would be expected from a "fold" in the i-front. These can be characterized by a "divergence index", p, with the value 2 for spherical flows and 1 for cylindrical flows.

Define r_s as the radius at which the photoevaporation flow shocks against the ambient gas of density n_0 (see Figure 5). This will be the point where the ram pressure of the photoevaporation flow is equal to the value of the thermal pressure of the ambient gas:

$$n_i \bar{m} c_i^2 \left(\frac{r_i}{r_s}\right)^p \frac{1 + M_s^2}{M_s} = n_0 \bar{m} c_i^2, \qquad (13)$$

where $\bar{m}$ is the mean mass per particle and M_s is the Mach number of the photoevaporation flow when it reaches the shock. Assuming the flow to be strictly isothermal, one can find the following implicit equation for M_s from the Bernoulli equation (e.g., Dyson 1968):

$$\frac{r_s}{r_i} = M_s^{-1/p} \exp\left(\frac{M_s^2 - 1}{2p}\right). \qquad (14)$$

The solutions of this equation for spherical and cylindrical flows are shown in Figure 6. It can be seen that the flow Mach number increases sharply at the base of the flow but is a rather shallow function of
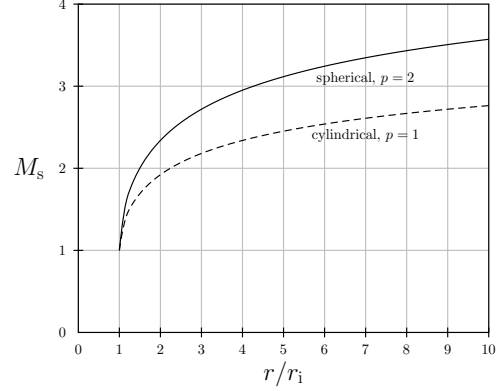

Fig. 6. Mach number as a function of radius for spherical and cylindrical isothermal photoevaporation flows. The radius is normalized to the radius of curvature of the i-front, r_i.

r beyond about 2 to 3 times the i-front radius, having a value $\simeq 2.5$ for cylindrical flows, and $\simeq 3$ for spherical flows.

The flow will hence carve out a cavity of radius r_s that is free of ambient gas, so that the ionizing photons that would have balanced the recombinations in the cavity can now be used to balance the recombinations in the photoevaporation flow instead. The rate of recombinations per unit area along the axis of the photoevaporation flow is given by

$$\Phi_{\text{flow}} = \alpha_B \int_{r_i}^{r_s} n^2 \, dr \equiv \omega_p r_i n_i^2 \alpha_B, \qquad (15)$$

where ω_p is the dimensionless "recombination thickness" of the flow, as in equation (2) above. From equation (12), the rate of recombinations per unit area at the i-front that would occur in the absence of the cavity is $\Phi_0 = \frac{4}{3}\pi R_0^3 n_0^2 \alpha_B / 4\pi R_0^2 = \frac{1}{3} R_0 n_0^2 \alpha_B$. The same rate for gas between the ionizing star and the shock position is $\Phi_{\text{inner}} = \frac{4}{3}\pi (R_0 - r_s)^3 n_0^2 \alpha_B / 4\pi R_0^2 = (1 - r_s/R_0)^3 \Phi_0$. The difference between these two must balance the recombinations in the photoevaporation flow: $\Phi_{\text{flow}} = \Phi_0 - \Phi_{\text{inner}}$, or

$$\omega_p r_i n_i^2 = \frac{1}{3}\left\{1 - \left[1 - \min\left(1, \frac{r_s}{R_0}\right)\right]^3\right\} R_0 n_0^2. \quad (16)$$

The dimensionless recombination thicknesses of cylindrical and spherical flows are given by $\omega_1 \simeq 0.30$ and $\omega_2 \simeq 0.12$, respectively. Using these, equations (13), (14), and (16) can be solved to find the cavity radius and density at the base of the flow as a function of the i-front radius of curvature. These solutions are shown in Figure 7. It can be seen that flows from quite small undulations can sustain cavities of a size comparable to the entire H II region:
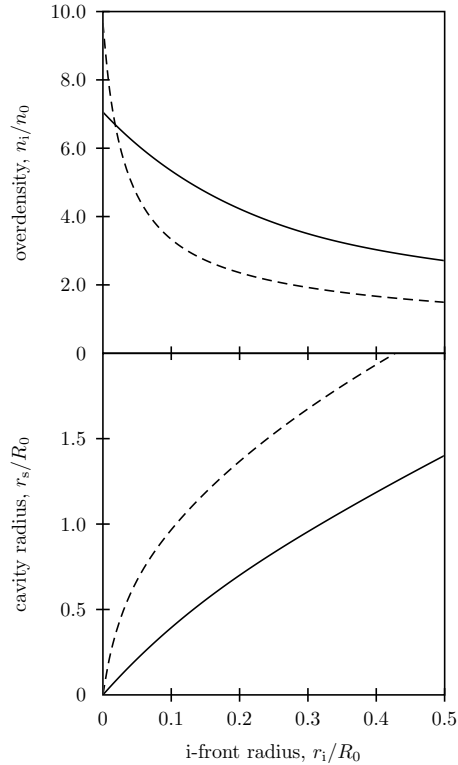
Fig. 7. The overdensity at the base of the flow and the size of the evacuated cavity for spherical (solid lines) and cylindrical (dashed lines) photoevaporation flows as a function of the radius of curvature of the i-front, r_i, normalized to the H II region radius, R_0.

$r_i \gtrsim 0.1$ (0.3) for cylindrical (spherical) flows, with base densities of a few times that in the homogeneous H II region. The surface brightness of such photoevaporation flows is proportional to the cavity radius and is therefore also comparable to that of the entire H II region. Flows from smaller undulations will have higher density (up to nearly $10n_0$ in the cylindrical case) but lower surface brightness.

4. APPLICATION TO THE ORION NEBULA

The detailed application of these models to observations of the Orion nebula will be presented elsewhere. Here, I briefly compare the predictions of the models with semi-empirical determinations of the geometry and physical parameters of the nebula, drawing on the observational work of Baldwin et al. (1991, B91) and Wen & O'Dell (1995, OW95).

B91 estimate the emission measure of the nebula (using the surface brightness of the hydrogen Paschen 11–3 line) at a series of positions from 2×10^{17} to 2×10^{18} cm to the west of the principal ionizing star, θ^1 Ori C. They combine this with estimates of the ionized density (from the [S II] doublet ratio, after correction for the partial ionization
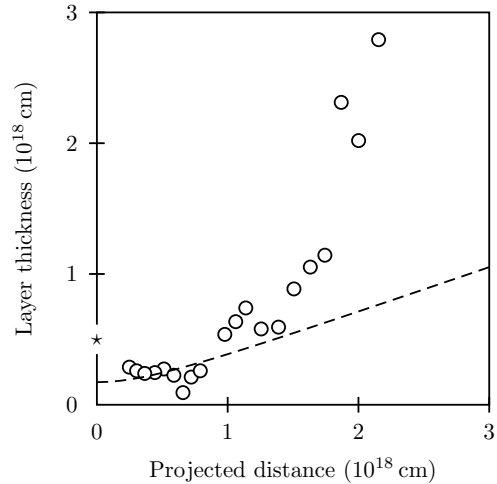

Fig. 8. Comparison of measurements of the thickness of the emitting layer in the Orion nebula (Baldwin et al. 1991—symbols) with predictions of the model of § 2 (dashed line).

in the [S II] emission zone) to calculate the effective thickness of the hydrogen line-emitting region as a function of position. OW95 carry this analysis a stage further by employing 2-D maps of the nebular surface brightness and density to reconstruct the emission layer thickness point-by-point over the entire face of the inner nebula within 10^{18} cm of θ^1 Ori C. Furthermore, they go on to use a simplified radiative transfer model to derive the 3-D shape of the i-front, finding that θ^1 Ori C lies at a distance $z_* \simeq 5 \times 10^{17}$ cm from the front. A NW-SE cut through their i-front solution shows a large-scale concave curvature but with a radius of curvature at least twice the distance between the i-front and the ionizing star. A NE-SW cut shows no pronounced curvature at the largest scale. Both cuts show irregularities with scales up to $r_i \simeq 3 \times 10^{17}$ cm, which correspond to the Orion bar and other similar features (e.g., O'Dell & Yusef-Zadeh 2000).

Figure 8 compares the B91 results for the emission layer thickness with the predictions from the model of the flow from a plane i-front (§ 2), assuming $z_* = 5 \times 10^{17}$ cm. The agreement is remarkably good within distances up to a few times z_* from the ionizing star.[2] Hence, it seems that the basic photoevaporation flow model can plausibly account for the gross-scale properties of the nebula. B91 invoked a static model for the nebula in which the strong gas pressure gradient in the emitting layer was balanced

_____

[2]At larger separations the observed thickness becomes significantly larger than what is predicted but, as noted above, the model assumptions are no longer valid there.

by the radiative force exerted on dust grains due to the absorption of starlight from θ^1 Ori C. However, such a model flies in the face of the well-established observational evidence that the ionized gas is flowing away from the molecular cloud at roughly sonic velocities (Kaler 1967; O'Dell et al. 1993; Henney & O'Dell 1999).

The model of § 3 can be directly compared with the Orion bar, which is the most prominent of several bright linear features (O'Dell & Yusef-Zadeh 2000), where the ionization front is seen tangentially to the line of sight. If these features represent photoevaporation flows from the crests of undulations in the i-front then they should show a higher density at the i-front than their surroundings. OW95 find just such a density increase (by a factor of about two) at the position of the bar. They interpret this as showing the density gradient *perpendicular to the i-front* in the emitting layer. However, this cannot be the case since their densities are based on the [S II] lines, whose emission is confined to a very thin layer ($\simeq 1 \times 10^{16}$ cm $\simeq 0.03h$) close to the i-front itself, and so the density gradient must be *along* the i-front. The bar lies at a projected distance of about 7×10^{16} cm from θ^1 Ori C, and its radius of curvature is about 2×10^{16} cm (assumed to be half the thickness of the bar in the sub-mm dust continuum maps of Johnstone & Bally 1999). Thus, $r_i/R_0 \simeq 0.3$ and, from Figure 7, the overdensity is predicted to be about two, as is observed. Another example of a convex undulation in the i-front is probably the brightest region of the nebula, located about 10^{17} cm to the SW of θ^1 Ori C, where the NS-oriented molecular ridge passes closest to the ionizing star. OW95 find that the emitting layer is at its thinnest ($h \simeq 5 \times 10^{16}$ cm) at this position. This is consistent with the flow from the crest of an undulation, where $h \simeq (0.12$ to $0.30)r_i$, as opposed to $0.346z_0$ in the flow from a plane i-front, implying a radius of curvature for the i-front of $r_i \simeq (1.5$ to $4) \times 10^{17}$ cm at that point, which is fully consistent with the shape reconstructed by OW95.

It is perhaps surprising that such simple models seem to work so well in reproducing the observations of the Orion nebula, which undoubtedly possesses a far more complex structure than is entertained here. The model of § 2 invoked many simplifying assumptions that need to be relaxed in a more realistic treatment, which should also take account of the shallow concavity shown by the i-front at large scales. The model of § 3 considers only the interaction of the small-scale flows with a homogeneous H II region, whereas it really should include the interaction with the large-scale flow that was modeled in § 2, as well as the mutual interactions between the undulations of various scales. Furthermore, the effects of radiation pressure, stellar winds, and mass loading by embedded proplyds should all be included in a more complete theory

Finally, the origin of the undulations in the i-front is an interesting problem that is beyond the scope of this paper but is discussed in detail in Williams (2003).

REFERENCES

Baldwin, J. A., et al. 1991, ApJ, 374, 580 (B91)

Bertoldi, F. 1989, ApJ, 346, 735

Dyson, J. E. 1968, Ap&SS, 1, 388

García-Segura, G., & Franco, J. 1996, ApJ, 469, 171

Henney, W. J. 2001, in 7th Texas-Mexico Conference on Astrophysics: Flows, Blows, & Glows, eds. G. Shields, W. H. Lee, & S. Torres-Peimbert, RevMexAA(SC), 10, 57

Henney, W. J., & O'Dell, C. R. 1999, AJ, 118, 2350

Henney, W. J., O'Dell, C. R., Meaburn, J., Garrington, S. T., & Lopez, J. A. 2002, ApJ, 566, 315

Hester, J. J., et al. 1996, AJ, 111, 2349

Johnstone, D., & Bally, J. 1999, ApJ, 510, L49

Kaler, J. B. 1967, ApJ, 148, 925

Moffat, A. F. J., et al. 2002, ApJ, 573, 191

O'Dell, C. R. 2001, ARA&A, 39, 99

O'Dell, C. R., Balick, B., Hajian, A. R., Henney, W. J., & Burkert, A. 2002, AJ, 123, 3329

O'Dell, C. R., Valk, J. H., Wen, Z., & Meyer, D. M. 1993, ApJ, 403, 678

O'Dell, C. R., & Yusef-Zadeh, F. 2000, AJ, 120, 382

Smith, N., Egan, M. P., Carey, S., Price, S. D., Morse, J. A., & Price, P. A. 2000, ApJ, 532, L145

Wen, Z. & O'Dell, C. R. 1995, ApJ, 438, 784 (WO95)

Walborn, N. R., & Maíz-Apellániz, J. 2002, AJ, 124, 1601

Williams, R. J. R. 2003, RevMexAA(SC), 15, 184 (this volume)

Williams, R. J. R., Ward-Thompson, D., & Whitworth, A. P. 2001, MNRAS, 327, 788

Yorke, H. W. 1986, ARA&A, 24, 49

William J. Henney: Instituto de Astronomía, Universidad Nacional Autónoma de México, Campus Morelia, Apartado Postal 3–72, 58090 Morelia, Michoacán, México (w.henney@astrosmo.unam.mx).